COBEM 2021 26th International Congress of Mechanical Engineering
November 22-26, 2021, Virtual Congress, Brazil

COB-2021-0994
Formation Guidance of Fully Actuated Multirotor Aerial Vehicles Using Global Sliding Modes

Jorge A. Ricardo Jr
Davi A. Santos
Aeronautics Institute of Technology, Praça Mal. Eduardo Gomes, 50 - Vila das Acácias, São José dos Campos - SP, 12228-900, Brazil
jorgejarj@ita.br
davists@ita.br

Abstract. *This paper investigates the robust position and attitude guidance of a group of fully actuated multirotor aerial vehicles equipped with fixed rotors and subject to bounded disturbances. To address the problem, we propose a hierarchical control architecture, in which a joint attitude-position flight control loop of each vehicle is nested inside the vehicle guidance loop. The flight control of each vehicle is designed using a proportional derivative strategy, while a global sliding mode strategy is adopted to robustly guide each vehicle in the presence of bounded disturbances. The latter ensures the robustness of the system from the initial time instant. The method is evaluated via numerical simulations using a formation of fully actuated hexacopters, showing to be effective and simple to implement and tune.*

Keywords: *multirotor aerial vehicle, global sliding mode control, formation guidance, nonlinear dynamics.*

1 INTRODUCTION

Many applications of multirotor aerial vehicles (MAVs), such as surveillance (Saska *et al.*, 2014) and agriculture monitoring (Mogili and Deepak, 2018), seem to benefit from the use of fully actuated MAVs due to its fast disturbance rejection (Jiang and Voyles, 2014) and independent attitude-position tracking. In general, a MAV has a reduced autonomy and payload capacity, which make complex tasks to be more effectively performed if a fleet of these vehicles is used instead. It turns out that flying a group of fully actuated MAVs in formation leads to a challenging control problem since it demands an accurate tracking performance of each vehicle in the presence of model uncertainties and disturbances.

Different formation control strategies have been reported in the literature, including behavior-based methods (Balch and Arkin, 1998), virtual structure techniques (Wang, 1991), and leader-follower schemes (Tan and Lewis, 1996). Among these strategies, the sliding mode control (SMC) has attracted a significant amount of attention. It uses a high-frequency switching control to drive the system output to the so-called sliding manifold, where the system ideally becomes insensitive to bounded-matched parametric uncertainties and disturbances. However, in real systems, the designed performance degrades due to the chattering phenomenon (Lee and Utkin, 2007), mainly caused by time discretization and unmodeled dynamics. The formation control of vehicles using first-order sliding mode techniques have been the subject of some recent researches (Defoort *et al.*, 2008; Dehghani and Menhaj, 2016; Thien and Kim, 2018). Particularly, Defoort *et al.* (2008) implements a leader-follower approach to a formation of autonomous robots using an integral SMC (Utkin and Shi, 1996), which guarantees the system insensitivity property during all time by enforcing a global sliding mode. In the same manner, Dehghani and Menhaj (2016) also uses a leader-follower approach for a formation of fixed-wing unmanned aircraft using an integral SMC, where the high-frequency control signal is filtered (by a first-order filter) to reduce chattering at the cost of losing robustness with respect to discontinuous disturbances. Thien and Kim (2018) proposes a decentralized formation control for a group of vehicles also using an integral SMC filtered by a first-order filter.

The present paper is concerned with the robust attitude-position tracking control of a formation of fully actuated MAVs equipped with fixed rotors. A hierarchical control architecture is proposed, in which the flight control loop of each MAV is nested inside its guidance loop. The flight control of each vehicle is designed using a proportional derivative strategy, and, motivated by the possibility of collision avoidance between the MAVs and bounded disturbance rejection during the whole movement, we design a guidance law based on a new global sliding mode control (GSMC). Differently from (Utkin and Shi, 1996), the proposed GSMC is formulated using the tracking error dynamics calculated with respect to a reference trajectory to eliminate the need for designing a time-varying sliding function. The formation attitude and position reference trajectories are designed using a second-order polynomial S-curve connecting the formation initial and desired poses. The remaining text is organized as follows. Subsection 1.1 presents the notation. Section 2 defines the problem and states the control objective. Section 3 presents the methodology, including the flight controller, the guidance law, and the formation reference trajectory shaping. Section 4 evaluates the method using numerical simulations. Finally, Section 5 concludes the paper.

1.1 NOTATION

Matrices and algebraic vectors are denoted, respectively, by uppercase and lowercase boldface letters, while geometric (Euclidian) vectors are denoted as in $\vec{a}$. A Cartesian coordinate system (CCS) is represented by the set $\mathcal{S}_b \triangleq \{B; \vec{x}_b, \vec{y}_b, \vec{z}_b\}$, with B representing its origin, and $\vec{x}_b$, $\vec{y}_b$, and $\vec{z}_b$ the unit geometric vectors along its orthogonal axes. The algebraic vectors corresponding to the projection of an arbitrary physical vector $\vec{a}$ onto $\mathcal{S}_b$ and $\mathcal{S}_g$ are denoted by $\mathbf{a}_b \in \mathbb{R}^3$ and $\mathbf{a}_g \in \mathbb{R}^3$, respectively. The relation between $\mathbf{a}_g$ and $\mathbf{a}_b$ is $\mathbf{a}_b = \mathbf{D}^{b/g}\mathbf{a}_g$, where $\mathbf{D}^{b/g} \in \mathrm{SO}(3)$ is the attitude matrix of $\mathcal{S}_b$ w.r.t. $\mathcal{S}_g$. The inverse of $\mathbf{D}^{b/g}$, which coincides with its transpose, is denoted by $\mathbf{D}^{g/b}$. The identity matrix of order n is denoted by $\mathbf{I}_n$. Consider the algebraic vector $\mathbf{a}_g$, its Euclidean norm and component-wise absolute value are denoted, respectively, by $||\mathbf{a}_g||$ and $|\mathbf{a}_g|$. A null vector and a vector of ones of arbitrarily dimension n are denoted, respectively, by $\mathbf{0}_n$ and $\mathbf{1}_n$. The standard unit (algebraic) vectors are denoted by $\mathbf{e}_1 \triangleq (1,0,0)$, $\mathbf{e}_2 \triangleq (0,1,0)$, and $\mathbf{e}_3 \triangleq (0,0,1)$. Let $\vec{a}^{\,b/g}$ represent am arbitrary relative physical quantity of $\mathcal{S}_b$ w.r.t. $\mathcal{S}_g$, *e.g.*, along the paper, $\vec{r}^{\,b/g}$ will denote the (relative) position of $\mathcal{S}_b$ w.r.t. $\mathcal{S}_g$. Finally, consider the $\mathcal{S}_g$ representations $\mathbf{a}_g \triangleq (a_1, a_2, a_3)$ and $\mathbf{b}_g$ of $\vec{a}$ and $\vec{b}$, respectively. The vector product $\vec{c} = \vec{a} \times \vec{b}$ is represented in $\mathcal{S}_g$ by $\mathbf{c}_g = [\mathbf{a}_g\times]\mathbf{b}_g$, where $[\mathbf{a}_g\times]$ is the following skew-symmetric matrix:

$$[\mathbf{a}_g\times] \triangleq \begin{bmatrix} 0 & -a_3 & a_2 \\ a_3 & 0 & -a_1 \\ -a_2 & a_1 & 0 \end{bmatrix}. \tag{1}$$

2 PROBLEM DEFINITION

Subsection 2.1 presents the position and attitude dynamic modeling of a fully actuated MAV equipped with fixed rotors and Subsection 2.2 presents the formation description and states the control objective.

2.1 EQUATIONS OF MOTION

Consider a formation of n fully actuated MAVs with fixed rotors. Let us define a ground-fixed CCS $\mathcal{S}_g \triangleq \{G; \vec{x}_g, \vec{y}_g, \vec{z}_g\}$, with G representing a known point on the ground, the ith MAV body-fixed CCS $\mathcal{S}_i \triangleq \{B_i; \vec{x}_i, \vec{y}_i, \vec{z}_i\}$, with B_i representing the ith MAV center of mass, and a formation reference CCS $\mathcal{S}_f \triangleq \{F; \vec{x}_f, \vec{y}_f, \vec{z}_f\}$, with F representing a formation reference point.

Considering $\mathcal{S}_g$ as an inertial CCS, the position dynamic model of the ith MAV is immediately obtained from the Newton's second law, being described in $\mathcal{S}_g$ by

$$\ddot{\mathbf{r}}_g^{\,i/g} = -g\mathbf{e}_3 + \frac{1}{m_i}\mathbf{f}_g^{\,c,i} + \frac{1}{m_i}\mathbf{f}_g^{\,d,i}, \tag{2}$$

where $\mathbf{r}_g^{\,i/g} \in \mathbb{R}^3$ is the $\mathcal{S}_g$ representation of the ith MAV position, $g \in \mathbb{R}$ is the gravity acceleration, $m_i \in \mathbb{R}$ is the ith MAV mass, and $\mathbf{f}_g^{\,c,i} \in \mathbb{R}^3$ and $\mathbf{f}_g^{\,d,i} \in \mathbb{R}^3$ are the $\mathcal{S}_g$ representations of the control and disturbance forces, respectively. The disturbance force $\mathbf{f}_g^{\,d,i}$ is unknown, but we assume that it is bounded according to

$$\left|\mathbf{f}_g^{\,d,i}\right| \leq \mathbf{f}_g^{\,i,\max}, \tag{3}$$

where $\mathbf{f}_g^{\,i,\max} \in \mathbb{R}^3$ is a given vector with positive components.

On the other hand, the attitude kinematics of $\mathcal{S}_i$ with respect to $\mathcal{S}_g$ are described in SO(3) by

$$\dot{\mathbf{D}}^{\,i/g} = -\left[\boldsymbol{\omega}_i^{\,i/g}\times\right]\mathbf{D}^{\,i/g}, \tag{4}$$

where $\mathbf{D}^{\,i/g} \in \mathrm{SO}(3)$ and $\boldsymbol{\omega}_i^{\,i/g} \in \mathbb{R}^3$ represent, respectively, the attitude and the $\mathcal{S}_i$ representation of the angular velocity of the ith MAV with respect to $\mathcal{S}_g$.

Using the Euler's equation, the attitude dynamics of the ith MAV are described in $\mathcal{S}_i$ by

$$\dot{\mathbf{h}}_i^{\,i} + \left[\boldsymbol{\omega}_i^{\,i/g}\times\right]\mathbf{h}_i^{\,i} = \boldsymbol{\tau}_i^{\,c,i} + \boldsymbol{\tau}_i^{\,d,i}, \tag{5}$$

where $\mathbf{h}_i^{\,i}$ is the $\mathcal{S}_i$ representation of the ith MAV angular momentum with respect to B_i, while $\boldsymbol{\tau}_i^{\,c,i} \in \mathbb{R}^3$ and $\boldsymbol{\tau}_i^{\,d,i} \in \mathbb{R}^3$ are, respectively, the $\mathcal{S}_i$ representations of the control and disturbance torques. The disturbance torque $\boldsymbol{\tau}_i^{\,d,i}$ is unknown, but we assume that it is bounded according to

$$\left|\boldsymbol{\tau}_i^{\,d,i}\right| \leq \boldsymbol{\tau}_i^{\,i,\max}, \tag{6}$$

where $\boldsymbol{\tau}_i^{i,\max} \in \mathbb{R}^3$ is given vector with positive components.

Neglecting the inertia properties of the spinning part of the rotors, the $\mathcal{S}_i$ representation of the ith MAV angular momentum can be expressed as

$$\mathbf{h}_i^i = \mathbf{J}_i^i \boldsymbol{\omega}_i^{i/g}, \tag{7}$$

where $\mathbf{J}_i^i \in \mathbb{R}^{3\times 3}$ is the inertia matrix of the ith MAV with respect to $\mathcal{S}_i$.

By replacing Eq. (7) into (5), the ith MAV attitude dynamics can be rewritten as

$$\dot{\boldsymbol{\omega}}_i^{i/g} = \left(\mathbf{J}_i^i\right)^{-1}\left[\mathbf{J}_i^i\boldsymbol{\omega}_i^{i/g}\times\right]\boldsymbol{\omega}_i^{i/g} + \left(\mathbf{J}_i^i\right)^{-1}\left(\boldsymbol{\tau}_i^{c,i} + \boldsymbol{\tau}_i^{d,i}\right). \tag{8}$$

2.2 CONTROL OBJECTIVE

Let us define the relative position and attitude of the ith MAV with respect to $\mathcal{S}_f$, respectively, by

$$\mathbf{r}_f^{i/f} \triangleq \mathbf{D}^{f/g}\left(\mathbf{r}_g^{i/g} - \mathbf{r}_g^{f/g}\right), \tag{9}$$

$$\mathbf{D}^{i/f} \triangleq \mathbf{D}^{i/g}\left(\mathbf{D}^{f/g}\right)^{\mathrm{T}}, \tag{10}$$

where $\mathbf{D}^{f/g}$ and $\mathbf{r}_g^{f/g}$ represent, respectively, the attitude and position of $\mathcal{S}_f$ with respect to $\mathcal{S}_g$. In this sense, the formation pose can be fully described by a set containing the pose of $\mathcal{S}_f$ with respect to $\mathcal{S}_g$ and the relative pose of all MAVs with respect to $\mathcal{S}_f$:

$$\mathcal{F}(t) = \left\{\mathbf{r}_g^{f/g},\, \mathbf{D}^{f/g},\, \left\{\mathbf{r}_f^{i/f},\, \mathbf{D}^{i/f}\right\}_{i=1}^{n}\right\}. \tag{11}$$

Let $\mathcal{S}_{\check{f}}$ and $\mathcal{S}_{\check{i}}$ denote the CCSs representing the desired orientation of $\mathcal{S}_f$ and $\mathcal{S}_i$, respectively. In the same manner, the desired formation pose, can be represented by the desired values of the elements of $\mathcal{F}$, *i.e.*,

$$\check{\mathcal{F}} = \left\{\check{\mathbf{r}}_g^{f/g},\, \check{\mathbf{D}}^{f/g},\, \left\{\check{\mathbf{r}}_f^{i/f},\, \check{\mathbf{D}}^{i/f}\right\}_{i=1}^{n}\right\}, \tag{12}$$

where

$$\check{\mathbf{r}}_f^{i/f} \triangleq \mathbf{r}_{\check{f}}^{\check{i}/\check{f}} \text{ and } \check{\mathbf{D}}^{i/f} \triangleq \mathbf{D}^{\check{i}/\check{f}}$$

are, respectively, the desired relative position and attitude of $\mathcal{S}_{\check{i}}$ with respect to $\mathcal{S}_{\check{f}}$, while

$$\check{\mathbf{r}}_g^{f/g} \triangleq \mathbf{r}_g^{\check{f}/g} \text{ and } \check{\mathbf{D}}^{f/g} \triangleq \mathbf{D}^{\check{f}/g}$$

are, respectively, the desired relative position and attitude of $\mathcal{S}_{\check{f}}$ with respect to $\mathcal{S}_g$.

Figure 1 illustrates the actual and desired poses of a formation composed by n fully actuated hexacopters.

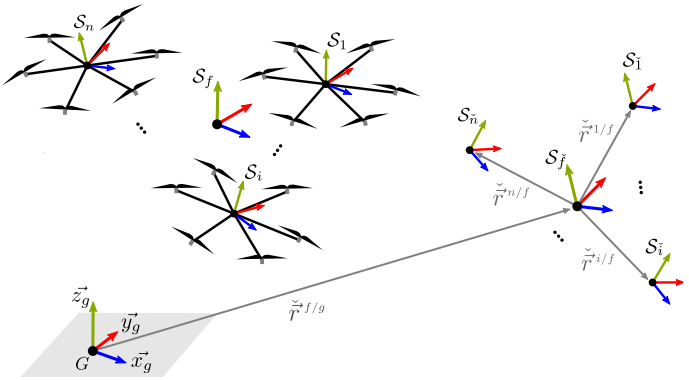

Figure 1. Schematic representation of a formation composed by n fully actuated hexacopters and its desired pose.

Given the definitions (11)–(12), the main problem of this paper can now be defined.

Problem 1. Design a flight control architecture to make $\mathcal{F} \to \check{\mathcal{F}}$ robustly with respect to the bounded disturbance force and torque.

3 PROBLEM SOLUTION

Subsection 3.1 proposes a control architecture for a formation of fully actuated MAVs equipped with fixed rotors to solve Problem 1. Subsection 3.2 presents the flight controller of each MAV. Subsection 3.3 derives the guidance law of each MAV. Finally, Subsection 3.4 presents the formation reference trajectory shaping.

3.1 HIERARCHICAL CONTROL ARCHITECTURE

The present paper adopts the hierarchical flight control architecture shown in Fig. 2. A cascade control structure is used for the ith MAV, where the flight control loop (inner loop i) is nested inside the guidance loop (outer loop i). In this architecture, the formation reference trajectory shaping receives the desired formation pose $\check{\mathcal{F}}$, and outputs the reference position trajectory $\hat{\mathbf{r}}_g^{i/g}$ and attitude trajectory $\hat{\mathbf{D}}^{i/g}$ to the guidance of the ith MAV. The latter receives the feedback of position, attitude, linear velocity, and angular velocity of the ith MAV to provide the commanded position $\bar{\mathbf{r}}_g^{i/g}$ and attitude $\bar{\mathbf{D}}^{i/g}$ to the flight control. Lastly, the flight controller also receives the feedback of position, attitude, linear velocity, and angular velocity of the ith MAV to generate the control force $\mathbf{f}_i^{i/g}$ and control torque $\boldsymbol{\tau}_i^{i/g}$.

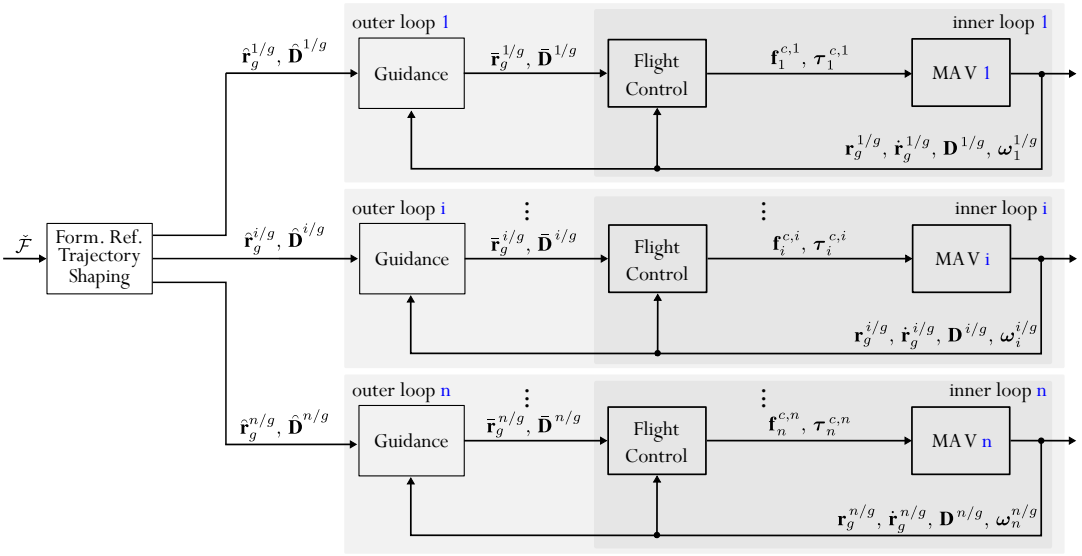

Figure 2. Proposed hierarchical flight control architecture for a formation composed of n fully actuated MAVs.

In the proposed hierarchical control architecture, the flight control law is designed to stabilize the MAV dynamics, while the guidance law is designed to guarantee the robustness of each MAV inner loop with respect to the bounded disturbances. Regarding the formation reference trajectory shaping, consider the following assumption.

Assumption 1. The reference position trajectory $\hat{\mathbf{r}}_g^{i/g}$ and attitude trajectory $\hat{\mathbf{D}}^{i/g}$ belong to the class $\mathcal{C}^k$, $\forall k \geq 1$ and connect the sets $\mathcal{F}(0)$ and $\check{\mathcal{F}}$.

Based on the proposed control architecture and Assumptions 1-, we can now divide Problem 1 into the following two subproblems, which, when fulfilled guarantees the formation robustness with respect to the bounded disturbances during all the time.

Subproblem 1.1. Design a flight control law to stabilize the ith MAV inner loop around $\bar{\mathbf{r}}_g^{i/g}$ and $\bar{\mathbf{D}}^{i/g}$.

Subproblem 1.2. Design a guidance law to ensure $\left(\mathbf{r}_g^{i/g}, \mathbf{D}^{i/g}\right) \equiv \left(\hat{\mathbf{r}}_g^{i/g}, \hat{\mathbf{D}}^{i/g}\right)$, $\forall t \geq 0$, in the presence of the bounded force and torque disturbances.

Different control techniques can be used to solve Subproblem 1.1 (see, *e.g.*, Silva and Santos, 2020), but specifically, in this paper we adopt a proportional derivative (PD) approach. On the other hand, Subproblem 1.2 can be effectively solved using a global sliding mode enabled by an adequate formation reference trajectory shaping satisfying Assumption 1.

As an important remark, consider the following assumption

Assumption 2. The reference position trajectories satisfies

$$\|\hat{\mathbf{r}}_g^{i/g} - \hat{\mathbf{r}}_g^{j/g}\| \leq \epsilon, \ \forall j = \{1, \ldots, n\} \backslash \{i\}, \tag{13}$$

where $\epsilon \in \mathbb{R}$ is a given safe distance between the MAVs.

If the formation reference trajectory shaping also satisfies Assumption 2, then a global sliding mode also guarantees the robustness of the system with respect to internal collisions during all the time. However, methods for fulfilling Assumption 2 are out of the scope of this paper and will appear in future work.

3.2 FLIGHT CONTROLLER

To stabilize the ith MAV, we adopt, respectively, the following PD position and attitude controllers

$$\mathbf{f}_g^{c,i} = m_i \left(g\mathbf{e}_3 + \mathbf{K}_1^i \left(\bar{\mathbf{r}}_g^{i/g} - \mathbf{r}_g^{i/g} \right) - \mathbf{K}_2^i \dot{\mathbf{r}}_g^{i/g} \right), \tag{14}$$

$$\boldsymbol{\tau}_i^{c,i} = -\left[\mathbf{J}_i^i \boldsymbol{\omega}_i^{i/g} \times \right] \boldsymbol{\omega}_i^{i/g} + \mathbf{J}_i^i \mathbf{K}_3^i \left(\bar{\mathbf{p}}^{\,i/g} - \mathbf{p}^{i/g} \right) - \mathbf{J}_i^i \mathbf{K}_4^i \boldsymbol{\omega}_i^{i/g}, \tag{15}$$

where $\mathbf{K}_j^i \in \mathbb{R}^{3\times 3}, \forall j = 1, \ldots, 4$ are diagonal gain matrices, $\mathbf{p}^{i/g} \in \mathbb{R}^3$ is the modified Rodrigues parameters (MRP) parameterizing $\mathbf{D}^{i/g}$, and $\bar{\mathbf{p}}^{i/g} \in \mathbb{R}^3$ is the MRP parameterizing $\bar{\mathbf{D}}^{i/g}$. The main advantage of using the MRP to represent the attitude command is that it allows rotations of up to 360 degrees. We highlight that this choice is consistent with a fully actuated MAV since it can perform larger angle maneuvers than an underactuated one.

The closed-loop dynamics, obtained by substituting (14) into (2) and (15) into (8), are given by

$$\ddot{\mathbf{r}}_g^{i/g} = -\mathbf{K}_1^i \mathbf{r}_g^{i/g} - \mathbf{K}_2^i \dot{\mathbf{r}}_g^{i/g} + \mathbf{K}_1^i \bar{\mathbf{r}}_g^{i/g} + \frac{1}{m_i} \mathbf{f}_g^{d,i}, \tag{16}$$

$$\dot{\boldsymbol{\omega}}_i^{i/g} = -\mathbf{K}_3^i \mathbf{p}^{i/g} - \mathbf{K}_4^i \boldsymbol{\omega}_i^{i/g} + \mathbf{K}_3^i \bar{\mathbf{p}}^{i/g} + \left(\mathbf{J}_i^i \right)^{-1} \boldsymbol{\tau}_i^{d,i}. \tag{17}$$

From Eqs. (16)–(17), one can show that, for bounded force and torque disturbances, the equilibrium point $(\bar{\mathbf{r}}_g^{i/g},\, \bar{\mathbf{p}}^{\,i/g}) \in \mathbb{R}^6$ is stable, thus fulfilling Subproblem 1.1.

3.3 GLOBAL SLIDING MODE GUIDANCE

Let us define the ith MAV position error with respect to the reference position trajectory

$$\tilde{\mathbf{r}}^{\,i/g} \triangleq \hat{\mathbf{r}}_g^{i/g} - \mathbf{r}_g^{i/g}. \tag{18}$$

The position error dynamic model is obtained by differentiating (18) twice and substituting (16) in the resulting expression, being given by

$$\ddot{\tilde{\mathbf{r}}}^{\,i/g} = \frac{d^2}{dt^2} \hat{\mathbf{r}}_g^{i/g} + \mathbf{K}_1^i \mathbf{r}_g^{i/g} + \mathbf{K}_2^i \dot{\mathbf{r}}_g^{i/g} - \mathbf{K}_1^i \bar{\mathbf{r}}_g^{i/g} - \frac{1}{m_i} \mathbf{f}_g^{d,i}. \tag{19}$$

Let us also define the ith MAV attitude and angular velocity errors with respect to the reference attitude trajectory, denoted respectively by $\tilde{\mathbf{D}}^{\,i} \in \mathrm{SO}(3)$ and $\tilde{\boldsymbol{\omega}}^{\,i} \in \mathbb{R}^3$, as

$$\tilde{\mathbf{D}}^{\,i} \triangleq \mathbf{D}^{i/\hat{i}}, \tag{20}$$

$$\tilde{\boldsymbol{\omega}}^{\,i} \triangleq \boldsymbol{\omega}_i^{i/\hat{i}}, \tag{21}$$

where $\hat{i}$ refers to the CCS representing the desired orientation for $\mathcal{S}_i$.

The control errors $\tilde{\mathbf{D}}^{\,i}$ and $\tilde{\boldsymbol{\omega}}^{\,i}$ can be put in the form (Ricardo Jr and Santos (2020))

$$\tilde{\mathbf{D}}^{\,i} = \mathbf{D}^{i/g} \left(\hat{\mathbf{D}}^{\,i/g} \right)^{\mathrm{T}}, \tag{22}$$

$$\tilde{\boldsymbol{\omega}}^{\,i} = \boldsymbol{\omega}_i^{i/g} - \tilde{\mathbf{D}}^{\,i} \hat{\boldsymbol{\omega}}_i^{\,i/g}, \tag{23}$$

where $\hat{\boldsymbol{\omega}}_i^{\,i/g}$ is the angular velocity of the reference trajectory.

From (22)–(23), the attitude error kinematics can be described in the same form as the full kinematics in (4), *i.e.*,

$$\dot{\tilde{\mathbf{D}}}^{\,i} = -\left[\tilde{\boldsymbol{\omega}}^{\,i} \times \right] \tilde{\mathbf{D}}^{\,i}. \tag{24}$$

We choose to parameterize $\tilde{\mathbf{D}}^{\,i}$, using the MRP (Markley and Crassidis, 2014)

$$\tilde{\mathbf{p}}^{\,i} \triangleq \tilde{\boldsymbol{\varepsilon}}^{\,i} \tan(\tilde{\vartheta}^{\,i}/4), \tag{25}$$

where $\tilde{\boldsymbol{\varepsilon}}^i \in \mathbb{R}^3$ and $\tilde{\vartheta}^i \in \mathbb{R}$ are, respectively, the principal Euler axis and angle corresponding to $\tilde{\mathbf{D}}^i$.

From (25), one can see that the MRP vector is singular at the angles $\tilde{\vartheta}^i = \pm(2z+2)\pi$ rad, $\forall z \in \mathbb{N}$. However, since the proposed attitude parameterization represents the attitude control error (not the full attitude), an effective design of the guidance law will keep $\tilde{\vartheta}^i$ smaller than 2π and singularities are not reached in practice.

The attitude error kinematics can be described using the MRP as

$$\dot{\tilde{\mathbf{p}}}^i = \frac{1}{4}\left(\left(1-\|\tilde{\mathbf{p}}^i\|^2\right)\mathbf{I}_3 + 2\left[\tilde{\mathbf{p}}^i\times\right] + 2\tilde{\mathbf{p}}^i\left(\tilde{\mathbf{p}}^i\right)^{\mathrm{T}}\right)\tilde{\boldsymbol{\omega}}^i. \tag{26}$$

The attitude error dynamics are obtained by differentiating (23) and substituting the closed-loop attitude dynamics (17) and the attitude error kinematics (24) in the resulting expression, being given by

$$\dot{\tilde{\boldsymbol{\omega}}}^i = -\mathbf{K}_3^i\mathbf{p}^{i/g} - \mathbf{K}_4^i\boldsymbol{\omega}_i^{i/g} + \mathbf{K}_3^i\bar{\mathbf{p}}^{i/g} + \left(\mathbf{J}_i^i\right)^{-1}\boldsymbol{\tau}_i^{d,i} - \tilde{\mathbf{D}}^i\hat{\boldsymbol{\omega}}_i^{i/g} + \left[\tilde{\boldsymbol{\omega}}^i\times\right]\tilde{\mathbf{D}}^i\hat{\boldsymbol{\omega}}_i^{i/g}. \tag{27}$$

Now, let us put the attitude error kinematics (26) and the error dynamics (19) and (27) into the simpler form

$$\dot{\mathbf{x}}_1^i = \mathbf{f}_1(\mathbf{x}_1^i, \mathbf{x}_2^i), \tag{28}$$

$$\dot{\mathbf{x}}_2^i = \mathbf{f}_2(\mathbf{x}_1^i, \mathbf{x}_2^i) + \mathbf{B}^i\mathbf{u}^i + \mathbf{G}^i\mathbf{d}^i, \tag{29}$$

by defining $\mathbf{x}_1^i \triangleq \left(\tilde{\mathbf{r}}^{i/g}, \tilde{\mathbf{p}}^i\right)$, $\mathbf{x}_2^i \triangleq \left(\dot{\tilde{\mathbf{r}}}^{i/g}, \tilde{\boldsymbol{\omega}}^i\right)$, $\mathbf{u}^i \triangleq \left(\bar{\mathbf{r}}_g^{i/g},\, \bar{\mathbf{p}}^{i/g}\right)$, $\mathbf{d}^i \triangleq \left(\mathbf{f}_g^{d,i},\, \boldsymbol{\tau}_i^{d,i}\right)$,

$$\mathbf{f}_1(\mathbf{x}_1^i, \mathbf{x}_2^i) \triangleq \begin{bmatrix} \dot{\tilde{\mathbf{r}}}^{i/g} \\ \frac{1}{4}\left(\left(1-\|\tilde{\mathbf{p}}^i\|^2\right)\mathbf{I}_3 + 2\left[\tilde{\mathbf{p}}^i\times\right] + 2\tilde{\mathbf{p}}^i\left(\tilde{\mathbf{p}}^i\right)^{\mathrm{T}}\right)\tilde{\boldsymbol{\omega}}^i \end{bmatrix},$$

$$\mathbf{f}_2(\mathbf{x}_1^i, \mathbf{x}_2^i) \triangleq \begin{bmatrix} \frac{d^2}{dt^2}\hat{\mathbf{r}}_g^{i/g} + \mathbf{K}_1^i\mathbf{r}_g^{i/g} + \mathbf{K}_2^i\dot{\mathbf{r}}_g^{i/g} \\ -\mathbf{K}_3^i\mathbf{p}^{i/g} - \mathbf{K}_4^i\boldsymbol{\omega}_i^{i/g} - \tilde{\mathbf{D}}^i\hat{\boldsymbol{\omega}}_i^{i/g} + \left[\tilde{\boldsymbol{\omega}}^i\times\right]\tilde{\mathbf{D}}^i\hat{\boldsymbol{\omega}}_i^{i/g} \end{bmatrix},$$

$$\mathbf{B}^i \triangleq \begin{bmatrix} -\mathbf{K}_1^i & \mathbf{0}_{3\times3} \\ \mathbf{0}_{3\times3} & \mathbf{K}_3^i \end{bmatrix},$$

$$\mathbf{G}^i \triangleq \begin{bmatrix} -\mathbf{I}_3/m_i & \mathbf{0}_{3\times3} \\ \mathbf{0}_{3\times3} & \left(\mathbf{J}_i^i\right)^{-1} \end{bmatrix}.$$

From the disturbance force and torque bounds, respectively defined in (3) and (6), the disturbance vector is bounded according to

$$\left|\mathbf{d}^i\right| \leq \mathbf{d}^{i,\max}, \tag{30}$$

where $\mathbf{d}^{i,\max} \triangleq \left(\mathbf{f}_g^{i,\max},\, \boldsymbol{\tau}_i^{i,\max}\right) \in \mathbb{R}^6$.

Let we define the sliding variable $\mathbf{s}^i \in \mathbb{R}^6$ of the ith MAV as

$$\mathbf{s}^i \triangleq \mathbf{x}_1^i + \mathbf{f}_1\left(\mathbf{x}_1^i, \mathbf{x}_2^i\right), \tag{31}$$

and the corresponding global sliding surface

$$\mathcal{S}^i \triangleq \left\{\left(\mathbf{x}_1^i,\, \mathbf{x}_2^i\right) \in \mathbb{R}^6 : \mathbf{s}^i = \mathbf{0}_6, \forall t \geq 0\right\}. \tag{32}$$

By differentiating (31) and using (28)–(29), we can obtain the dynamic equation of $\mathbf{s}^i$ (we omit the function independent variables for simplicity) as

$$\dot{\mathbf{s}}^i = \mathbf{f}_1 + \frac{\partial\mathbf{f}_1}{\partial\mathbf{x}_1}\mathbf{f}_1 + \frac{\partial\mathbf{f}_1}{\partial\mathbf{x}_2}\mathbf{f}_2 + \frac{\partial\mathbf{f}_1}{\partial\mathbf{x}_2}\mathbf{B}^i\mathbf{u}^i + \frac{\partial\mathbf{f}_1}{\partial\mathbf{x}_2}\mathbf{G}^i\mathbf{d}^i. \tag{33}$$

The following lemma gives a multi-input SMC law that enforces a global sliding mode of system (28)–(29) on $\mathcal{S}^i$.

Lemma 1. The control law

$$\mathbf{u}^i = -\left(\frac{\partial\mathbf{f}_1}{\partial\mathbf{x}_2^i}\mathbf{B}^i\right)^{-1}\left(\mathbf{f}_1 + \frac{\partial\mathbf{f}_1}{\partial\mathbf{x}_1^i}\mathbf{f}_1 + \frac{\partial\mathbf{f}_1}{\partial\mathbf{x}_2^i}\mathbf{f}_2 + \mathbf{K}^i\mathrm{sign}(\mathbf{s}^i)\right), \tag{34}$$

where $\mathbf{K}^i \in \mathbb{R}^{6\times6}$ is a constant diagonal gain matrix satisfying

$$\mathbf{K}^i\mathbf{1}_6 = \left|\frac{\partial\mathbf{f}_1}{\partial\mathbf{x}_2^i}\mathbf{G}^i\right|\mathbf{d}^{i,\max} + \boldsymbol{\delta}^i, \tag{35}$$

with $\boldsymbol{\delta}^i \in \mathbb{R}^6$ representing a given vector with positive components, guarantees the global sliding mode of system (28)–(29) on $\mathcal{S}^i$.

Proof. Consider the Lyapunov function candidate $V(\mathbf{s}^i) = 0.5(\mathbf{s}^i)^{\mathrm{T}}\mathbf{s}^i$. From Assumption 1, the system (28)–(29) is already on the sliding surface at $t = 0$ s. Then, to prove the global sliding mode of the system (28)–(29) on $\mathcal{S}^i$ it is sufficient to show that $\dot{V} < 0$, $\forall \mathbf{s}^i \neq \mathbf{0}_6$. Differentiating $V(\mathbf{s}^i)$, substituting (33)–(34), and choosing $\mathbf{K}^i$ according to (35), we can obtain

$$
\begin{aligned}
\dot{V}(\mathbf{s}^i) &= -(\mathbf{s}^i)^{\mathrm{T}} \left(\mathbf{K}^i \mathrm{sign}(\mathbf{s}^i) - \frac{\partial \mathbf{f}_1}{\partial \mathbf{x}_2^i} \mathbf{G}^i \mathbf{d}^i \right), \\
&= -\left|(\mathbf{s}^i)^{\mathrm{T}}\right| \mathrm{diag}(\mathrm{sign}(\mathbf{s}^i)) \left(\mathbf{K}^i \mathrm{sign}(\mathbf{s}^i) - \frac{\partial \mathbf{f}_1}{\partial \mathbf{x}_2^i} \mathbf{G}^i \mathbf{d}^i \right), \\
&= -\left|(\mathbf{s}^i)^{\mathrm{T}}\right| \left(\mathbf{K}^i \mathbf{1}_6 - \mathrm{diag}(\mathrm{sign}(\mathbf{s}^i)) \frac{\partial \mathbf{f}_1}{\partial \mathbf{x}_2^i} \mathbf{G}^i \mathbf{d}^i \right), \\
&\leq -\left|(\mathbf{s}^i)^{\mathrm{T}}\right| \left(\left| \frac{\partial \mathbf{f}_1}{\partial \mathbf{x}_2^i} \mathbf{G}^i \right| \mathbf{d}^{i,\max} + \boldsymbol{\delta}^i - \mathbf{I}_6 \left| \frac{\partial \mathbf{f}_1}{\partial \mathbf{x}_2^i} \mathbf{G}^i \right| \mathbf{d}^{i,\max} \right), \\
&\leq -\left|(\mathbf{s}^i)^{\mathrm{T}}\right| \boldsymbol{\delta}^i < 0, \; \forall \mathbf{s}^i \neq \mathbf{0}_6,
\end{aligned}
$$

to prove the global sliding mode of system (28)–(29) on $\mathcal{S}^i$.

3.4 FORMATION REFERENCE TRAJECTORY SHAPING

This section proposes a formation reference trajectory shaping based on a second-order polynomial S-curve model. The trajectories connect the formation initial pose $\mathcal{F}(0)$ to the desired formation set $\check{\mathcal{F}}$, thus fulfilling Assumption 1, and contain three sequential phases: acceleration, cruise, and deceleration.

Let us define the following states

$$\mathbf{z}_1^i \triangleq \hat{\mathbf{r}}_g^{f/g} - \mathbf{r}_g^{f/g}(0), \tag{36}$$

$$\mathbf{z}_2^i \triangleq \hat{\mathbf{r}}_g^{i/f} - \mathbf{r}_g^{i/f}(0), \tag{37}$$

$$\mathbf{z}_3^i \triangleq \boldsymbol{\alpha}^{i/\hat{i}}, \tag{38}$$

where $\boldsymbol{\alpha}^{i/\hat{i}} \in \mathbb{R}^3$ is any three-dimensional attitude parameterization of the attitude error $\mathbf{D}^{i/g}(0)\hat{\mathbf{D}}^{g/i}$.

The states $\mathbf{z}_j^i$, $\forall j = 1, \ldots, 3$, receive as parameters the trajectory time period t_j and the desired displacements $\mathbf{z}_1^i(t_1) \triangleq \check{\mathbf{r}}_g^{f/g} - \mathbf{r}_g^{f/g}(0)$, $\mathbf{z}_2^i(t_2) \triangleq \check{\mathbf{r}}_g^{i/f} - \mathbf{r}_g^{i/f}(0)$, and $\mathbf{z}_3^i(t_3) \triangleq \boldsymbol{\alpha}^{i/\check{i}}$. The time instants t_1, t_2, and t_3 represent, respectively, the time of the formation position trajectory, the time to achieve the desired formation shape, and the vehicles attitude trajectory time.

For simplicity, we consider that the acceleration, cruise, and deceleration phases have the same duration. In this sense, the second time derivative of the states $\ddot{\mathbf{z}}_j^i$, $\forall j = 1, \ldots, 3$ are given by the following piece-wise constant function

$$\ddot{\mathbf{z}}_j^i = \begin{cases} \ddot{\mathbf{z}}_j^{i,\max}, & 0 \leq t < t_j/3 \\ \mathbf{0}_3, & t_j/3 \leq t < 2t_j/3 \\ -\ddot{\mathbf{z}}_j^{i,\max}, & 2t_j/3 \leq t \leq t_j \end{cases} \tag{39}$$

where $\ddot{\mathbf{z}}_j^{i,\max}$ is the maximum acceleration, calculated from $\ddot{\mathbf{z}}_j^{i,\max} = 4.5\mathbf{z}_j^i(t_j)/t_j^2$. Figure 3 shows the motion profile of the first component of $\mathbf{z}_j^i$.

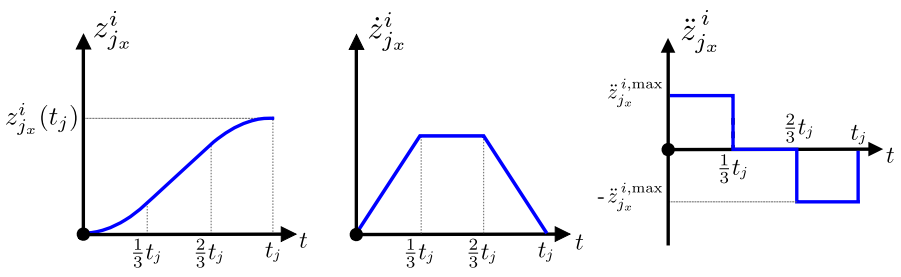

Figure 3. Second-order polynomial S-curve trajectory with equal duration phases.

The reference position and attitude trajectory of the ith MAV are calculated from the states $\mathbf{z}_j^i$, respectively as

$$\hat{\mathbf{r}}_g^{i/g} = \mathbf{z}_1^i + \mathbf{z}_2^i + \mathbf{r}_g^{i/g}(0), \tag{40}$$

$$\hat{\mathbf{D}}^{i/g} = \left(\mathbf{D}^{i/\hat{i}}\right)^{\mathrm{T}} \mathbf{D}^{i/g}(0), \tag{41}$$

where $\mathbf{D}^{i/\hat{i}}$ is the attitude matrix calculated from the chosen three-dimensional attitude parameterization $\alpha^{i/\hat{i}}$.

We highlight that the presented methodology is easy to implement since the reference trajectories are analytically calculated from the integration of (39).

4 NUMERICAL SIMULATION

To perform the simulational study, the proposed methodology is applied to a formation of non-planar fully actuated hexacopters equipped with fixed rotors. The simulation, coded in MATLAB, is performed using a time step of 0.001 s and uses the Euler integration method. The actuator dynamics are implemented in the simulation and are a relevant source of chattering in sliding mode controllers.

The formation is composed by three identical MAVs and its parameters are presented in Table 1, where $\check{\boldsymbol{\alpha}}^{i/f} \triangleq (\check{\phi}^{i/f}, \check{\theta}^{i/f}, \check{\psi}^{i/f})$ is the 123 Euler angles attitude parameterizing $\check{\mathbf{D}}^{i/f}$.

Table 1. Formation parameters.

Description	Symbol	Value
Desired position of $\mathcal{S}_f$ w.r.t.$\mathcal{S}_g$	$\check{\mathbf{r}}_g^{f/g}$	$(4,\ 6,\ 10)$ m
Desired attitude of $\mathcal{S}_f$ w.r.t. $\mathcal{S}_g$	$\check{\mathbf{D}}^{f/g}$	$\mathbf{I}_3$
Desired position of MAV-1 w.r.t. $\mathcal{S}_f$	$\check{\mathbf{r}}_f^{1/f}$	$(0,\ 0,\ 0)$ m
Desired position of MAV-2 w.r.t. $\mathcal{S}_f$	$\check{\mathbf{r}}_f^{2/f}$	$(1.4142,\ -1.4142,\ 0)$ m
Desired position of MAV-3 w.r.t. $\mathcal{S}_f$	$\check{\mathbf{r}}_f^{3/f}$	$(-2,\ 0,\ 0)$ m
Desired attitude of the ith MAV w.r.t. $\mathcal{S}_f$ in 123 Euler angles	$\check{\boldsymbol{\alpha}}^{i/f}$	$(20,\ 5,\ 10)$ deg

The ith MAV has a total mass $m^i = 1\,\mathrm{kg}$, arm length of 0.5, and inertia matrix $\mathbf{J}_i^i = \mathrm{diag}(0.015, 0.015, 0.015)$ kgm^2. The vehicles initial positions are $\mathbf{r}_g^{1/g} = (0,\ 0,\ 0)$ m , $\mathbf{r}_g^{2/g} = (-1,\ -1,\ 0)$ m , and $\mathbf{r}_g^{3/g} = (-2,\ -2,\ 0)$ m. The duration of the formation position trajectory is $t_1 = 9\,\mathrm{s}$. The time to obtain the formation shape is $t_2 = 3\,\mathrm{s}$ and the MAVs attitude trajectory duration is $t_3 = 5\,\mathrm{s}$. In this sense, the MAVs will obtain a delta-shaped formation at $t = 3\,\mathrm{s}$ and keep it along the whole position trajectory. Moreover, the ith MAV is subjected to the disturbance $\mathbf{d}^i = \boldsymbol{\nu}\cos\left(t + (i-1)\pi/2\right)$, where $\boldsymbol{\nu} \triangleq (-0.6,\ 0.5,\ -0.4,\ -0.1,\ 0.08,\ -0.05)$.

The GSMC gain matrix of each MAV is $\mathbf{K}^i = \mathrm{diag}(1.32,\ 1.1,\ 0.88,\ 17.33,\ 13.33,\ 10.67)$. On the other hand, the PD flight controller gain matrices of each MAV are $\mathbf{K}_1^i = \mathbf{I}_3$, $\mathbf{K}_2^i = 2\mathbf{I}_3$, $\mathbf{K}_3^i = 3\mathbf{I}_3$, and $\mathbf{K}_4^i = 3\mathbf{I}_3$.

Figure 4 shows, in plot (a), the formation path, the formation shape at the time instants 0, 3, 6, and 9 s along with circles representing the MAVs size, while plot (b) shows the norm of the relative position between MAV 1 and MAVs 2 and 3, denoted, respectively, by $\mathbf{r}_g^{1/2}$ and $\mathbf{r}_g^{1/3}$. It can be seen that the formation shape is obtained at $t = 3\,\mathrm{s}$ and maintained during the rest of the movement.

Figure 5 shows the position plots for the MAV 2. It shows the MAV position tracking performance, the position command, and the control force. In the plots, we see a precise tracking of the position reference trajectory with no relevant chattering and the high-frequency position command and control force. On the other hand, Fig. 6 shows the attitude plots for the MAV 2. It shows the attitude tracking performance, the attitude command, and the control torque. In the plots, we see an oscillatory motion of the attitude variables around the reference trajectory and the high-frequency attitude command and control torque. Chattering is more evident in Fig. 6 (a) than in Fig. 5 (a) since the attitude dynamics are faster than the position dynamics, being more influenced by the discretization process and the actuator unmodeled dynamics.

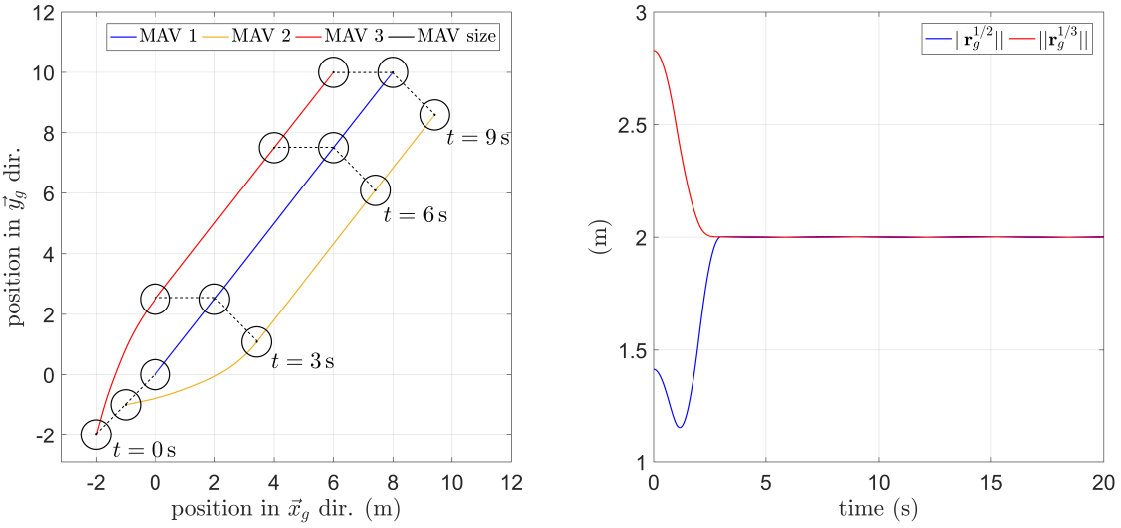

(a) (b)

Figure 4. Formation plots. (a): Formation path, formation shape at the time instants 0, 3, 6, and 9 s along with circles representing the MAVs size. (b): Norm of the relative position between MAV 1 and MAVs 2 and 3.

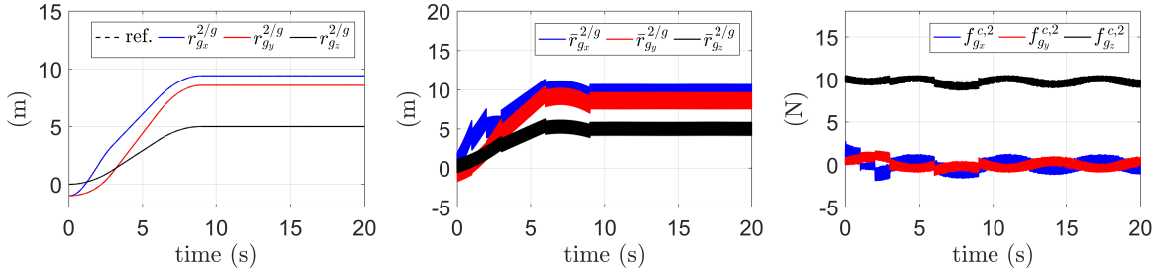

(a) (b) (c)

Figure 5. Position plots of MAV 2. (a): Position tracking performance. (b) Position command. (c) Control force.

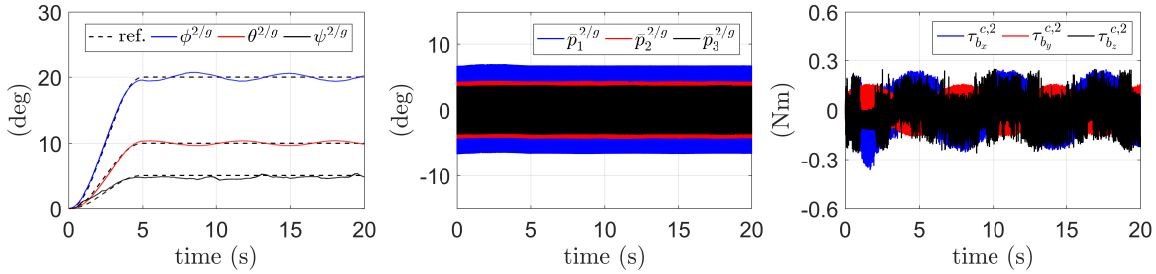

(a) (b) (c)

Figure 6. Attitude plots of MAV 2. (a): Attitude tracking performance. (b) Attitude command. (c) Control torque.

5 CONCLUSIONS

This paper solved the position and attitude tracking problem for a general formation of fully actuated MAVs equipped with fixed rotors using a guidance law, based on a global SMC that guarantees the robustness of each MAV with respect to bounded disturbances during all the time. The global sliding mode existence is proved using Lyapunov stability theory. Moreover, the proposed formation reference trajectory shaping allows specifying the time duration of the formation position and attitude trajectories, as well as the trajectory time duration needed to achieve the formation shape from an initial condition. A simulation example showed the effectiveness and promising performance of the method.

6 ACKNOWLEDGEMENTS

The authors would like to thank the Sao Paulo Research Foundation (FAPESP), for the financial support (2019/05334-0). The first author is grateful to EMBRAER and ITA, for the doctorate scholarship under the Academic-Industrial Graduate Program (DAI), and to CNPq/Brazil for the doctorate scholarship. The second author is grateful for the support of CNPq/Brazil (302637/2018-4).

7 REFERENCES

Balch, T. and Arkin, R., 1998. "Behavior-based formation control for multirobot teams". *IEEE Transactions on Robotics and Automation*, Vol. 14, No. 6, pp. 926–939.

Defoort, M., Floquet, T., Kokosy, A. and Perruquetti, W., 2008. "Sliding-mode formation control for cooperative autonomous mobile robots". *Industrial Electronics, IEEE Transactions on*, Vol. 55, pp. 3944 – 3953.

Dehghani, M.A. and Menhaj, M.B., 2016. "Integral sliding mode formation control of fixed-wing unmanned aircraft using seeker as a relative measurement system". *Aerospace Science and Technology*, Vol. 58, pp. 318–327.

Jiang, G. and Voyles, R., 2014. "A nonparallel hexrotor uav with faster response to disturbances for precision position keeping". *IEEE International Symposium on Safety, Security, and Rescue Robotics*, pp. 1–5.

Lee, J. and Utkin, V., 2007. "Chattering suppression methods in sliding mode control systems". *Annual Reviews in Control*, Vol. 31, pp. 179–188.

Markley, F.L. and Crassidis, J.L., 2014. *Fundamentals of Spacecraft Attitude Determination and Control*. Space Technology Library. Springer-Verlag, New York.

Mogili, U.R. and Deepak, B.B.V.L., 2018. "Review on Application of Drone Systems in Precision Agriculture". *Procedia Computer Science*, Vol. 133, pp. 502–509.

Ricardo Jr, J.A. and Santos, D.A., 2020. "Attitude tracking control for a quadrotor aerial robot using adaptive sliding modes". *Ibero-Latin-American Congress on Computational Methods in Engineering*.

Saska, M., Chudoba, J., Přeučil, L., Thomas, J., Loianno, G., Třešňák, A., Vonásek, V. and Kumar, V., 2014. "Autonomous deployment of swarms of micro-aerial vehicles in cooperative surveillance". *2014 International Conference on Unmanned Aircraft Systems (ICUAS)*, pp. 584–595.

Silva, A.L. and Santos, D.A., 2020. "Fast nonsingular terminal sliding mode flight control for multirotor aerial vehicles". *IEEE Transactions on Aerospace and Electronic Systems*, Vol. 56, No. 6, pp. 4288–4299. doi: 10.1109/TAES.2020.2988836.

Tan, K.H. and Lewis, M.A., 1996. "Virtual structures for high-precision cooperative mobile robotic control". *Proceedings of IEEE/RSJ International Conference on Intelligent Robots and Systems. IROS '96*, Vol. 1, pp. 132–139.

Thien, R.T. and Kim, Y., 2018. "Decentralized formation flight via pid and integral sliding mode control". *IFAC-PapersOnLine*, Vol. 51, No. 23, pp. 13–15.

Utkin, V. and Shi, J., 1996. "Integral sliding mode in systems operating under uncertainty conditions". In *Proceedings of 35th IEEE Conference on Decision and Control*. Vol. 4, pp. 4591–4596 vol.4. doi:10.1109/CDC.1996.577594.

Wang, P.K.C., 1991. "Navigation strategies for multiple autonomous mobile robots moving in formation". *Journal of Robotic Systems*, Vol. 8, No. 2, pp. 177–195.

8 RESPONSIBILITY NOTICE

The authors are solely responsible for the printed material included in this paper.